JOURNAL OF GLACIOLOGY

CAMBRIDGE UNIVERSITY PRESS

Temporal Variability in Snow Accumulation and Density at Summit Camp, Greenland Ice Sheet

	surface mass balance reanalysis models significantly underestimate accumulation rates at Summit Camp. This is concerning because such models are often used to estimate ice sheet mass loss.

SCHOLARONE™
Manuscripts

1 **TEMPORAL VARIABILITY IN SNOW ACCUMULATION AND DENSITY AT SUMMIT CAMP,**

2 **GREENLAND ICE SHEET**

3 Ian Howat

4 Byrd Polar and Climate Research Center & School of Earth Sciences

5 The Ohio State University

6

7

8

9

10

11

12

13

14

15

16

17

18

1

19   **ABSTRACT**

20   A three-year record of weekly snow water equivalent (SWE) accumulation at Summit Camp,

21   central Greenland Ice Sheet, obtained by direct sampling, is presented. While the overall SWE

22   accumulation of 24.2 cm w.e. a^{-1} matches long-term ice core estimates, variability increases at

23   shorter time scales. Half of the annual SWE accumulation occurs during a few large events, with

24   the average accumulation rate decreasing 35% between the first and second halves of the record

25   coinciding with exceptional anticyclonic conditions in the spring and summer of 2019. No

26   seasonality in accumulation is detected. Rather, local accumulation rates appear to be

27   significantly impacted by wind redistribution that obscures temporal patterns in snowfall. Surface

28   snow density is consistent, on average, with previously measured values but does not correlate

29   with near surface temperature or wind speed. Two surface mass balance reanalysis models

30   significantly underestimate accumulation rates at Summit Camp. This is concerning because such

31   models are often used to estimate ice sheet mass loss.

32

33

34

35

36

37

38

39

1. INTRODUCTION

The surface mass balance (SMB) of the Greenland Ice Sheet is, primarily, the difference between the mass gained through snowfall and that lost due to melt runoff (Lenaerts and others, 2019). Greenland's annual SMB has declined over the past three decades due to increased melting relative to snowfall. The rates of iceberg calving and melting at the ice/ocean interface have also increased, resulting in an increasingly negative total mass balance and an increasing contribution to sea level rise (IMBIE Team, 2019). Snowfall accumulation is the single largest term in the Greenland ice sheet mass budget and has the largest interannual variability (Box and others, 2013; Gallagher and others, 2022). Accumulation is also highly complex since it is dependent on both large-scale atmospheric circulation and local-scale surface processes, including wind redistribution. The characteristics of accumulated snow also change quickly through time by multiple metamorphic processes that are also dependent on atmospheric conditions. Understanding and predicting accumulation, therefore, requires detailed observations of snow and firn at a wide range of spatial and temporal scales (Lenaerts and others, 2019).

Much of our understanding of the mass of snow accumulation on ice sheets comes from relatively sparse measurements from ice cores, snow pits, or inferences based on remotely sensed data. These are limited to, typically, annual resolution or, in the case of remotely sensed data, subject to significant uncertainties regarding snow density, grain size or other physical properties required to estimate mass accumulation (McIlhattan and others, 2020). No direct measurements of mass accumulation and near-surface density on ice sheets at higher temporal resolution over multiple years are known to exist. This is because of the logistical challenges of obtaining field measurements. There is, therefore, a critical gap in direct observations of mass accumulation and surface density at the temporal scale of atmospheric and surface variability which are necessary for process understanding. Further, such measurements provide valuable ground truth for remote sensing. For example, the success of satellite altimetry missions, such as ICESat-2, is dependent

65   on the ability to obtain estimates of ice sheet mass balance from changes in surface elevation,

66   thus requiring knowledge of the density of the accumulation and the changes in firn density that

67   contribute to surface height changes. Additionally, atmospheric reanalysis models, another

68   primary source for ice sheet mass balance estimates and forcing for firn models used to correct

69   altimetry measurements (e.g., Kuipers Munneke and others, 2015), rely on ground measurements

70   for calibration and validation. As such, the ability of these models for representing accumulation

71   is not well constrained (Fettwies and others, 2020; Montgomery and others, 2020). Due to the

72   vastness of ice sheet interiors, small biases in the rate of surface accumulation can cause large

73   errors in mass balance. For example, a 1 cm a^{-1} bias in the rate of annual water-equivalent

74   accumulation over the Greenland Ice Sheet equates to 15 Gt a^{-1} of mass, or over 5% of the current

75   rate of loss (IMBIE, 2019).

76   Located at the highest point of the interior Greenland Ice Sheet and occupied year-round for over

77   twenty years, Summit Camp provides a unique platform for supporting observational campaigns

78   that require frequent and sustained manual measurements, equipment maintenance and

79   sheltered laboratory facilities. These include detailed measurements of a wide range of

80   atmospheric variables (e.g., Box and Steffen, 2001; Castellani et al. 2015; Berkelhammer et al.,

81   2016), snow accumulation (e.g. Dibbs and Fahnestock, 2003) and firn density (e.g., Zwally and

82   Li, 2002). As a result, much of our understanding of large-scale processes and atmospheric

83   drivers controlling Greenland's accumulation comes from observations at Summit Camp. Yet, a

84   sustained program of measuring mass accumulation and surface density through time had not

85   been undertaken.

86   To fill this observational gap and provide a benchmark dataset for instrument calibration and

87   validation, measurements of changes in the mass and thickness of surface accumulation were

88   obtained manually at approximately seven-day intervals for three years at Summit Camp. These

89   measurements provide unprecedented information about temporal variability in surface mass

90   accumulation and surface snow density.

91   While a preliminary version of the first year of these observations was shown in Howat and others,

92   (2018), the full three-year dataset is presented here, including quality control and errors. The

93   observations are then used to examine temporal variability in snow water-equivalent accumulation

94   and density at various time scales and in relation to local meteorology. Finally, the mass

95   accumulation estimates are compared to concurrent measurements of snow height change at a

96   network of stakes, snowfall observed by ground-based Doppler radar, and accumulation rates

97   predicted by two ice sheet surface mass balance reanalysis models often used for estimating ice

98   sheet mass changes.

99   **2. SNOW BOARD MEASUREMENTS**

100   Observations of accumulation thickness, snow water equivalent (SWE) thickness and density

101   were obtained using the snow board method, where accumulation atop a board, which serves as

102   a depth reference, is repeatedly sampled and measured. The snow board method has been used

103   for over a century to measure mountain snowpack (e.g., Wayand and others. 2015), but no

104   application to measuring ice sheet accumulation was found in the literature. A shallow, rectangular

105   pit is excavated, and a piece of plywood is placed over the floor of the pit. The pit is then allowed

106   to fill with snow and settle over a period of at least two weeks. A plastic tube is used to remove a

107   core sample of the snow from the surface to the plywood, which serves as a depth reference for

108   each subsequent sample. The sample is taken from a different location on the board each time,

109   as measured from flagged poles at the corner of the plywood, to provide an undisturbed sample.

110   The snow water equivalent (SWE) of the sample is obtained from both its mass and water volume,

111   providing redundancy for quality control. To obtain the SWE thickness of the sample from its

112   mass, the sample is brought indoors in its sampling tube and weighed. The weight of the empty

113   sampling tube is subtracted, and this weight is divided by the cross-sectional area of the tube. To

114   obtain the SWE thickness from the sample volume, the sample is allowed to melt and the liquid

115   volume is divided by the cross-sectional area of the core. The snow depth at each sampling site

116   is also recorded. The SWE estimate divided by this depth gives an estimate of sample density.

117   Measurement precisions and resulting uncertainties are provided in the Supplementary Material.

118   When no undisturbed locations remain on the board, or the snow becomes too deep to sample,

119   sampling moves to a new, adjacent snow board site. During the change to a new site, samples

120   are taken at the same time at both the old and new site. These are termed tie points. Subtracting

121   the SWE value of the tie point at the new site from that of the old site, and adding this difference

122   to later measurements, gives the cumulate change in SWE across site transitions. The snow

123   board sampling sites were in a designated area of undisturbed snow, upwind of other field

124   instrumentation and buildings to minimize their influence on accumulation.

125   A total of 147 measurements were recorded between 7 March 2017 and 5 March 2020, averaging

126   7 ±2 days between surveys (Fig. 1). Measurements of snow depth ranged from 8 cm to 58 cm,

127   with a mean of 26.7 cm ±11.9 cm. Survey sites were occupied 90 days, on average, with the

128   longest being 141 days from 5 Jun to 24 October 2019. The shortest, 29 days, was the final site.

129   SWE observations obtained from sample mass ranged from 2.62 to 18.40 cm w.e., averaging

130   8.00 cm w.e. and with a standard deviation of ±3.43 cm w.e.. On average, SWE derived from

131   mass was 0.05 cm w.e., or 0.75%, less than that derived from volume, with the root-mean-square

132   of differences equaling 0.15 cm w.e. (note this was mistakenly reported as 1.5 cm w.e. in Howat

133   and others, 2018), or 1.9% and with 95% of measurements within 0.31 cm w.e. or 3.2% (Fig. S1).

134   The disagreement between mass and volume measurements tends to increase with sample size,

135   with a standard deviation of 0.11 cm w.e. below 10 cm w.e. and 0.21 cm w.e. above, and no

136   measurements agree within 0.2 cm w.e. for samples over 14 cm w.e.. This indicates some

137 unknown instrumental or procedural error in larger samples, and it is not known whether this

138 impacts mass, volume or both measurements. A description of dataset quality control is provided

139 in the Supplementary Material.

FIGURE 1 NEAR HERE

140 **3. RESULTS**

141 Subtracting differences between concurrent tie-point measurements at sample site transitions

142 provides an estimate of the cumulative SWE thickness over the 3-year record (Fig. 2a). Total

143 SWE accumulation was 69.5 $\pm$0.2 cm w.e. for an average rate of 24.2 cm w.e. a^{-1}, equal within

144 uncertainty to the long-term annual rate of 24 cm w.e. obtained from the GISP ice core (Alley and

145 others, 1993). Subtracting this average trend from the time series (Fig. 2b), there is no clear

146 seasonality. Instead, the time series is dominated by multi-year variability punctuated by distinct

147 periods of increasing and decreasing accumulation. Following a sustained period of declining

148 SWE between May and August 2017, the rate of accumulation was approximately one third

149 greater than the mean between October 2017 and January 2019. The accumulation rate then

150 declined to two thirds of the mean from January 2019 through the rest of the record. Overall, the

151 accumulation rate of 28.6 cm a^{-1} during the first half of the record was 35% greater than the 18.6

152 cm a^{-1} during the second half. This interannual variability appears to be a consequence of more

153 frequent, large accumulation events in 2017 and 2018. Out of the six measurements of increased

154 accumulation greater than 3 cm w.e. per seven days, five occur before April 2018, with the sixth

155 in October 2018 (Fig. 2c). These large increases are typically followed by rapid declines of 1 to 2

156 cm w.e over the following one to three measurements. However, two significant seven-day

157 declines of 1.5 and 1 cm w.e. occur on 22 May 2019 and 16 January 2020, respectively, that were

158 not preceded by accumulation events.

159   One quarter of the observations recorded a decrease in SWE from the previous measurement.

160   The 10th and 90th percentiles of the seven-day change in SWE were -0.36 cm and 1.60 cm,

161   respectively, with a maximum gain of 4.01 cm, or one-sixth the annual accumulation, between 2

162   and 9 November 2017, followed closely by the maximum observed loss of 2.33 cm between 15

163   and 22 November 2017. Increases greater than the 90th percentile accounted for 50% of the total

164   cumulative SWE. Over the record, declines in SWE totaled 16.60 cm, or 24% of the cumulative

165   total, with half of that loss occurring in the first year when overall accumulation rates were larger.

166   Density obtained by dividing sample SWE by snow depth ranged from 0.201 g cm^{-3} to 0.441 g

167   cm^{-3} with a mean of 0.303 g cm^{-3} and a standard deviation of $\pm$ 0.044 g cm^{-3} (Fig. 2d). This is

168   nearly identical to the average of 0.305 g cm^{-3} measured by Dibb and Fahnestock (2004) for the

169   upper 1 m at Summit Camp, and slightly less than the average of 0.315 g cm^{-3} for 10 cm depth

170   from 200 measurements from across Greenland (Fausto and others, 2018). The time series of

171   density shows three sharp minima in January 2018, October 2018 and August 2018, with less

172   defined maxima between. The highest densities, reaching over 0.4 g cm^{-3} occur at the transfer

173   from the first to second snow board site in July 2017, which were measured from samples with

174   thicknesses less than 10 cm. Density then decreased to the January 2018 minimum of 0.21 g

175   cm^{-3}. The lowest recorded density of 0.20 g cm^{-3} on 15 August 2019 was observed during a period

176   of high variability. Overall, density declined by -0.022 g cm^{-3} per year. However, excluding the

177   period of anomalously high densities and lower sample depths before 15 August 2017, the trend

178   declines by nearly half, to -0.012 g cm^{-3} per year.

179   Interpretation of the density record recovered from the snow board samples is complicated by the

180   varying sample depth. Density should vary, in part, as a function of sample snow depth as deeper

181   samples will tend to include older snow that has undergone more metamorphism. Conversely, as

182   mentioned above, thinner samples may include a larger fraction of wind packed surface layers of

183   high density. However, the plot of density and snow depth (Fig. 3) shows no consistent

8

184 relationship. As shown previously, densities are highest for the thinnest snow depths measured

185 between 20 June and 22 August 2017. Other periods with nearly as thin snow depths, however,

186 do no not have anomalously high densities, indicating that the anomaly was specific for that time

187 period. The most variability in density occurs for snow depths between 18 and 22 cm. While

188 maximum densities remain consistent at ~0.350 g cm^{-3} across snow depths above 10 cm,

189 minimum densities decline to below 0.24 g cm^{-3} within this depth range.

190 FIGURE 2 NEAR HERE

191 FIGURE 3 NEAR HERE

192 This high variability in sample density indicates an inconsistent relationship between changes in

193 snow depth and changes in SWE. Changes in SWE between measurements are plotted against

194 changes in snow depth in Fig. 4. Three outliers with values greater than three standard deviations

195 from the best fit line occur in September and November 2017. The November 2017 outliers occur

196 when snow depths are the highest recorded, at over 50 cm. As described in Section 2, samples

197 from the largest snow depths may have larger errors. The 27 September 2017 outlier occurred

198 earlier at the sampling site during a period of rapid accumulation, but it's unclear if this

199 measurement is erroneous. Removing these outliers, changes in snow thickness correspond to

200 61% of the variability in SWE with an average density equivalent of 0.278 g cm^{-3}. Using this

201 density, predicting changes in SWE from changes in sample thickness would give a root-mean-

202 square error of 0.52 cm w.e., or 106% the average change in SWE between seven-day

203 observations. However, the fractional error in SWE estimated from snow thickness change tends

204 to decrease with time. After one year, the cumulative thickness scaled by the average density

205 (0.278 g cm^{-3}) is 1.70 cm w.e., or less than 6% of the observed 29.49 cm w.e.. This fractional

206 difference remains near 5% for the remainder of the record. Therefore, if a long-term mean

207 surface density can be established and compaction can be accounted for, this suggests that SWE

208   may be estimated from changes in accumulation thickness to a precision comparable to the snow

209   board measurement precision (e.g., ±3%). This estimate may be improved through statistical

210   modeling, such as applied to seasonal snow by Sturm and others (2010).

211   FIGURE 4 NEAR HERE

212   **4. COMPARISON TO METEOROLOGICAL OBSERVATIONS**

213   Meteorological variables including air temperature 2m above the surface, wind speed, wind

214   direction and barometric pressure have been recorded by the U.S. National Oceanic and

215   Atmospheric Administration (NOAA) at an automatic weather station at Summit Camp nearly

216   continuously since 2008. Hourly data were obtained from the NOAA Earth System Research

217   Laboratory Global Monitoring Division data portal (https://gml.noaa.gov/aftp/data/meteorology/in-

218   situ/sum/, Last Accessed: 21 November 2021). Daily and 30-day retrospective means are

219   compared to the snow board observations of detrended cumulative SWE accumulation and

220   density in Figs. S2 and S3 in the Supplementary Material.

221   The decrease in accumulation rate between April and August 2019 corresponds with sustained

222   high pressure, with a 30-day retrospective average value reaching 687 hPa. This value is greater

223   than the 99th percentile over the 2008 to 2021 meteorological record and was a major ablation

224   event throughout Greenland (Tedesco and Fettweis, 2019). The largest decrease in SWE (-1.6

225   cm w.e.) between observations occurred between 22 and 28 May 2019, when daily average

226   pressure reached near 700 hPa. It's unclear what caused this decrease, as wind speeds were

227   depressed to below 5 m s^{-1} and temperatures were -10°C or less. This rate is far greater than

228   could be attributed to sublimation (Box and Steffen, 2001).

229   The highest wind speeds observed since 2008 occurred January and February 2018, with a 30-

230   day average reaching 11 m s^{-1} and a peak speed of 21.7 m s^{-1} on 23 February 2018. Another

231   period of high winds occurred at the end of the record, with a 30-day mean reaching 9.3 m s^{-1} on

232   1 February 2020. Neither of these periods of anomalous winds corresponded with anomalies in

233   SWE accumulation. Overall, mean wind speed between snow board observations explains only

234   ~5% of the variability in accumulation. Additionally, there is no apparent correlation between

235   accumulation and wind direction, as previously detected for snowfall (Castellani and others,

236   2015).

237   Density is expected to vary with air temperature and pressure, which closely track each other at

238   Summit Station, through crystal grain growth in the atmosphere and rates of dry snow

239   metamorphism in the snowpack (e.g., Zwally and Li, 2002; Fausto and others, 2018). Wind should

240   also play a role in controlling turbulent heat and vapor fluxes at the surface. Comparing the density

241   record to daily averaged surface air temperature and wind speed, however, reveals no consistent

242   relationship (Fig. S3). Over the first 18 months, density tracks air temperature and pressure, falling

243   from the highest observed values between 20 June and 22 August 2017, to a minimum January

244   2018, and then rising and falling with temperature and pressure through October 2018. After this

245   period, however, variations in density decouple from air temperature and pressure, showing little

246   or no seasonal cycle. Conversely, density does not appear to track wind speed in the first half of

247   the record, with highs in density occurring, generally, during periods of lower wind speed. After

248   October 2018, however, density appears to vary with wind speed, declining during a period of

249   lower wind speeds during summer 2019, and then increasing in tandem at the end of the record.

250   Variations in density vary weakly (r^2=0.06) but significantly (p=0.005) with the 30-day mean wind

251   direction, increasing in density as winds move from the southeast (130°) to southwest (210°). A

252   possible explanation for this correlation may be snowfall type. Pettersen and others (2018) found

253   that southeasterly winds correspond with precipitation from ice clouds, whereas southwesterly

254   winds correspond with snowfall from warmer, mixed-phase clouds.

255   **5. COMPARISON TO THE "BAMBOO FOREST" SNOW STAKE NETWORK**

1

256 As with any point measurement, it is uncertain how representative the snow thickness

257 measurements at the snow board sampling sites are to the greater Summit Camp region.

258 Variations in surface height have been measured at a network of snow stakes, nicknamed "The

259 Bamboo Forest", at Summit Camp continuously since 2003. As with the snow board snow

260 thickness measurements, these stakes record changes in surface accumulation and ablation, but

261 also record compaction between the surface and the base of the stakes (Dibb and Fahnestock,

262 2004). Therefore, if the changes in snow thickness are equivalent between the snow board site

263 and the bamboo forest, they should display the same short-term variations, but increasingly

264 diverge by amount equal to the increased compaction rate at the stakes relative to the snow

265 board.

266 Snow   stake   data   are   obtained   from   the   Summit   Camp   data   repository

267 (https://conus.summitcamp.org, last accessed: 21 November 2021). The cumulative stake height

268 change is obtained from the average change of individual stake measurements. The cumulative

269 change in snow depth of the snow board samples is plotted with cumulative change in stake

270 height in Fig. 5. While the two records have similar short-term variations, they increasingly

271 diverge, with the snowboard measurements becoming increasingly greater than the snow stake

272 measurements at an average rate of 15.12 cm a^{-1}. Such a trend is expected as the snow stakes

273 record both the amount of accumulation and the surface lowering due to densification between

274 the surface and the base of the stakes (Dibb and Fahnestock, 2014). A compaction rate of 15.12

275 cm a^{-1} is consistent with field measurements and modeling (Dibb and Fahnestock, 2014).

276 Adjusting the snow stake record for compaction by adding the trend of 15.12 cm a^{-1} results in a

277 close match with the snow board record (Fig. 5b), yielding a root-mean-square of differences of

278 4.0 cm, well within the snow stake standard deviation of 8.2 cm. As expected, the average of the

279 snow stake measurements has a smaller magnitude of short-term variability than the point

280 measurement provided by the snow board. Notably, the short-term minima in snow depth change

281 averaged from the snow stakes on 10 August 2017 and 28 July 2019 were 6.0 and 4.0 cm less,

282 respectively, than the snow board. Additionally, several short-term peaks in snow depth change

283 are visible in the snow board record that are not reflected in the snow stake average, particularly

284 a sustained increase of up to 7.4 cm between October 2018 and February 2019. Thus, this

285 comparison suggests that the snow board measurements are broadly representative of the larger

286 Summit Camp area, when additionally accounting for snow compaction. Short term (monthly or

287 less) variability, however, may reflect local conditions within the range expected from the

288 individual snow stake measurements.

289 FIGURE 5 NEAR HERE

290 **6. COMPARISON TO THE PRECIPITATION OCCURRENCE SENSOR SYSTEM**

291 SWE accumulation reflects variations in both snowfall and wind redistribution. To separate these

292 contributions, the snow board accumulation record is compared to snowfall measured by the

293 precipitation occurrence sensor system (POSS). The POSS is a continuous wave, X-band

294 Doppler radar deployed at Summit Camp as part of the Integrated Characterization of Energy,

295 Clouds, Atmospheric state, and Precipitation at Summit (ICECAPS) project (Sheppard and Joe,

296 2008; Castellani and others, 2015). The POSS samples approximately one cubic meter of air

297 directly above the transmitter and receiver, providing observations of near-surface precipitation

298 type, amount, and frequency, in liquid water equivalent. Hourly snowfall rates are obtained from

299 NOAA   Physical   Sciences   Laboratory

300 (ftp://ftp1.esrl.noaa.gov/psd3/arctic/summit/poss/processed/, last accessed 21 November 2021).

301 The instantaneous water equivalent snowfall rates measured by the POSS are converted into

302 cumulative SWE to compare to the snow board SWE record (Fig. 6a). We note that because the

303 POSS only records snowfall, and not ablation, we would expect it to estimate a greater

304 accumulation than the snow board. Cumulative POSS snowfall, however, is 21.2 cm w.e. over

305   the three-year period, or less than a third of the 69.5 cm w.e. measured from the snow board,

306   remaining between 26 and 33% of the snow board measurement after the first year. Castellani

307   and others (2015) suggested that underestimation of accumulation by the POSS, compared to

308   the snow stake network in that case, may be mostly due to biases in the calibration used for

309   converting reflectivity to the snowfall.

310   FIGURE 6 NEAR HERE

311   Subtracting the trend from each time series (Fig. 6b), there is little or no agreement in sub annual

312   variability. Consistent with Bennartz and others (2019), the POSS shows seasonal peaks in

313   snowfall rate in August and September of 2017 and 2018. However, no such peak is visible in

314   2019, which was the summer of persistent anticyclonic conditions over central Greenland

315   (Tedesco and Fettweis, 2019).

316   At the time scale of individual observations, there is a weak (r^2=0.08) but significant (p=10^{-3})

317   correlation between changes in POSS cumulative snowfall and changes in snowboard cumulative

318   SWE (Fig. 6c). No loss in SWE between snowboard observations occurred when the change in

319   cumulative snowfall was greater than 4 mm w.e., with all losses greater than 1 cm occurring when

320   cumulative snowfall was near zero. Large increases in SWE at the snow board, however, do not

321   appear correlated with cumulative snowfall, with anomalously large (> 2 cm w.e.) increases in

322   SWE occurring with cumulative snowfalls of 3 mm w.e. or less.

323   **7. COMPARISON TO ATMOSPHERIC REANALYSIS MODEL ESTIMATES**

324   Atmospheric reanalysis models are widely used to provide estimates of surface accumulation and

325   ice sheet mass balance. The snow board measurements provide a rare opportunity to validate

326   model estimates for changes in SWE, which is equivalent to surface mass balance (SMB) on ice

327   sheets, at high temporal resolution over multiple years. The snow board SWE measurements are

328 compared to two regional reanalysis models with openly available output for ice sheet

329 accumulation: the Modern Era Retrospective analysis for Research and Applications version 2

330 (MERRA-2) (Gelaro and others, 2017) and the Modèle Atmosphérique Régional (MAR) (Fettweis

331 and others, 2013).

332 MERRA-2 Land Ice Surface Diagnostics estimates are provided by NASA Global Modeling and

333 Assimilation Office (GMAO) using the Goddard Earth Observing System Model (GEOS) version

334 5.12.4 (GMAO, 2015). MERRA-2 contains a snow process model that tracks surface mass and

335 heat fluxes (Cullather and others, 2014). The model output, posted at 0.5° by 0.625° resolution,

336 includes 3-hourly estimates of the total mass of the snow and firn layer, which are differenced to

337 provide the SMB in water equivalent thickness. The time series of cumulative SWE at the snow

338 board location is obtained through bilinear interpolation of the 3-hourly grids to the snow board

339 coordinates. Since the time of the snow board observation was not recorded, we compare

340 cumulative MERRA-2 SWE values obtained at noon UTC of each day to the snowboard

341 measurements in Fig. 7a. For the 3-year observation period, MERRA-2 predicts an average

342 accumulation rate of 20.0 cm w.e. a^{-1}, or 18% less than that from the snow board observations.

343 MAR version 3.12 is obtained from the Climate Center at Liege University

344 (ftp://ftp.climato.be/fettweis/MARv3.12, last accessed: 8 February 2022). It has a 10-km

345 resolution, daily output forced by the ERA5 reanalysis model. As with MERRA-2, MAR contains

346 a dynamic ice sheet surface and snow/firn layer model. MAR provides a daily estimate of SMB

347 as a standard product. These are summed between snow board measurements to provide an

348 estimate of the total change in SWE. As with MERRA2, MAR predicts a substantially lower rate

349 of accumulation than observed, averaging 18.8 cm w.e. a^{-1} and totaling 55.31 cm w.e., or 20%

350 less than observed with the snow board.

351 Removing the trend from both series (Fig. 7b) reveals that MERRA-2 and MAR capture much of

352 the inter-annual and shorter-term variability, including the multiple single accumulation events,

353 such as on 19 May and 6 November 2017, and 16 July 2018. Overall, MERRA-2 and MAR

354 account for 75% and 70% of the variability in SWE. For MERRA-2, the root-mean-square error in

355 changes between measurements of 0.82 cm w.e. per seven days, and 1.43 cm w.e. for the

356 cumulative change in the detrended time series. For MAR, these are 0.85 cm w.e. per seven

357 days, and 1.67 cm for cumulative change in the detrended time series.

358 FIGURE 7 NEAR HERE

359 Spatial variability likely contributes to the differences between the snow board observations and

360 reanalysis model estimates. The timing and magnitude of the differences in detrended series in

361 Fig. 7b appear similar to those between the snow board and snow stake snow depth changes

362 plotted in Fig. 5b. The detrended reanalysis model estimates and the cumulative change in SWE

363 estimated from the snow stake average snow depth using a density 0f 0.3 g cm^{-3}, are plotted in

364 Fig. 7c. These show a closer agreement in sub annual variability than the snow board

365 observations, with the snow stakes accounting for 87% and 79% of the variability in MERRA-2

366 and MAR, respectively, and seven-day root-mean-square errors of 0.30 and 0.33 cm w.e.,

367 respectively. This indicates that a significant portion of the sub annual differences between snow

368 board and reanalysis model estimates are due to spatial variability, which is better characterized

369 by the spatially extensive snow stake network. However, the bias in average annual SWE

370 accumulation rates is the same as with the snow board observations. Using the compaction rate

371 of 15.12 cm a^{-1} estimated in Section 5 and a density of 0.3 g cm^{-3}, the snow stakes give an average

372 annual SWE accumulation rate of 24.48 cm a^{-1}.

373 **8. CONCLUSIONS**

374 The first long-term, continuous, and direct measurements of snow water equivalent accumulation

375 on the Greenland Ice Sheet reveal increasing variability at shorter timescales. While the three-

376 year average annual accumulation is identical to the multi-decade average obtained from ice

377 cores, year-to-year accumulation varied by over one-third of the average rate over the period of

378 observation. This is larger than the maximum annual change of ~25% between 1974 and 1975

379 measured from a series of shallow cores spanning 1964 to 1987 around Summit Camp (Bolzan

380 and Stroebel, 1994). The reduction in accumulation rate was concurrent with exceptionally strong

381 and persistent anticyclonic conditions in the spring and summer of 2019 (Tedesco and Fettweis,

382 2019) that was reflected in extremely high atmospheric pressure, lasting for several months at

383 Summit Camp. While Summit Camp receives approximately half its snowfall from mixed-phase

384 clouds originating from the southwest under anticyclonic conditions in the summer (Petterson and

385 others, 2018; McIlhattan and others, 2020), the 2019 event was anomalous in its pattern of

386 sustained northerly flow, resulting in decreased snowfall in the interior ice sheet (Tedesco and

387 Fettweis, 2019). This is apparent in the POSS measurements, which showed a greatly diminished

388 seasonal peak in snowfall in summer of 2019 relative to the previous years. The fact that the

389 three-year mean is near the expected long-term average suggests anomalously high

390 accumulation rates prior to 2019; the average accumulation rate was 28.33 cm w.e. a^{-1} from March

391 2017 to December 2018.

392 Consistent with Dibb and Fahnestock (2004), and despite multiple studies finding a seasonal

393 cycle in snowfall (Bennartz and others, 2019), we find no evidence for a consistent annual cycle

394 in accumulation at Summit Camp. Rather, the time series is dominated by the interannual

395 variability described above and individual accumulation events throughout the year that could be

396 due to snowfall and/or wind redistribution. Half of the accumulation was deposited in large events,

397 mostly in 2017 and 2018, where the seven-day accumulation rate exceeded the 90th percentile

398 and which individually were a substantial fraction (> 10%) of the annual accumulation. Despite

399 the co-occurrence of decreased accumulation and persistent high pressure in 2019, and the

400 expectation for snowfall to correlate with southerly winds (Cullather and others 2014; Petterson

401 and others, 2018; Gallagher and others, 2022), weekly accumulation rates do not significantly

402 correlate with average surface wind direction or pressure. Conversely, cumulative mass losses,

403 which exceed 1 cm w.e. in seven days, are equivalent to nearly a quarter of the total mass gain.

404 This loss is much larger than could be accounted for by sublimation (Box and Steffen, 2001) and,

405 therefore, must be due to wind erosion and redistribution.

406 Local, short-term rates of wind erosion are lacking (Lenaerts and others, 2012), but several

407 observations point to the importance of wind redistribution in controlling local accumulation. First

408 is the lack of temporal correlation between accumulation and snowfall recorded by the POSS,

409 which shows the expected late summer peak (Bennartz and others, 2019). This indicates another

410 process regulates how a snowfall is accumulated. At weekly time scales, however, the POSS

411 reveals that losses in SWE are larger during periods with lower cumulative snowfall, suggesting

412 that snowfall does counter net erosion. Second, short-term differences in accumulation between

413 the snow board and the snow stake network, as well as within the network itself, demonstrate

414 significant spatial variability indicative of erosion and/or redistribution through transport in the air

415 columns and/or drifting. Third, periods of greatest mass loss tended to follow large accumulation

416 events, when wind erosion is expected to be fastest due to the low density of new snowfall

417 (Lenaerts and others, 2012). Despite this evidence, there is no clear correlation between average

418 wind speed and weekly accumulation, indicating a more complex relationship that is potentially

419 dependent on surface winds, snow density, relative humidity, and drifting, all operating on even

420 shorter timescales than the snow board observations.

421 The density of the surface accumulation showed variability of 10 to 20% on time scales ranging

422 from weeks to years. Consistent with Fausto and others (2019), there is not a clear correlation

423 with surface wind speed or temperature. On weekly timescales, due to these variations in density,

424 changes in snow thickness account for only 60% of the change in mass. However, thickness

425 changes become more representative of mass changes when differencing over longer periods of

426　time, so that, assuming a standard surface density of ~0.3 g cm^{-3}, gives an estimate of mass

427　change within 5% after one year. Good agreement between snow depth change recorded at the

428　snow board and the snow stake network average is achieved by accounting for compaction at a

429　constant rate of 15.12 cm a^{-1}, consistent with a previous estimate (Dibb and Fahnestock, 2014),

430　indicating that variability at the snow board provides a representative measurement of the larger

431　region on annual timescales and, conversely, mass accumulation can be estimated from the snow

432　stake measurements at high relative accuracy at annual or longer timescales using these mean

433　values for compaction rate and density.

434　Finally, the snow board measurements reveal substantial (18% and 20%) underestimates of

435　accumulation by two prominent meteorological reanalysis models. This indicates a model bias

436　towards too little snowfall in the Summit Camp region. Bennartz and others (2019) found a similar

437　underestimate in snowfall accumulation in the ERA-Interim reanalysis model for Summit Camp

438　when compared to that estimated from CloudSat cloud-profiling radar satellite observations

439　calibrated with ground-based radar. They attributed this bias to the model not capturing shallow,

440　more convective precipitation in the summer months, Additionally, using airborne snow

441　penetrating radar, Overly and others (2016) and Montgomery and others (2020) have detected

442　underestimates of over 40% in reanalysis model snowfall estimates in western and southeastern

443　Greenland, respectively. Therefore, this may be a widespread bias that could significantly bias

444　mass balance estimates; a 20% bias in the 700 Gt a^{-1} accumulation rate (Box and others, 2013)

445　would represent about 50% of the current rate of mass loss (IMBIE, 2020). However, with the

446　multi-year trend removed, the reanalysis models capture much of the variability in accumulation

447　on inter-annual and shorter time scales, suggesting that assessments of temporal variability using

448　these models are more robust.

449　The Summit Camp snow board data used in this study are available at:

450　https://doi.org/10.5061/dryad.f7m0cfxz9

451 **SUPPLEMENTARY MATERIAL**

452 The supplementary material for this article can be found in the accompanying file

453 "SupplementaryMaterial.pdf".

454 **ACKNOWLEDGEMENTS**

460

461

462

463

464

465

466

467

468

469

470

471

472

473

474

REFERENCES

Alley R, Meese D, Shuman C, Gow A, Taylor K, Grootes P, White J, Ram M, Waddington E, Mayewski P and Zielinski G (1993) Abrupt Increase in Greenland Snow Accumulation at the End of the Younger Dryas Event. *Nature,* **362**(6420), 527-529 (doi: 10.1038/362527a0)

Bennartz R, Fell F, Pettersen C, Shupe MD and Schuettemeyer D (2019) Spatial and temporal variability of snowfall over Greenland from CloudSat observations*. Atmospheric Chemistry and Physics,* **19**(12), 8101-8121 (doi: 10.5194/acp-19-8101-2019)

Berkelhammer M, Noone DC, Steen-Larsen HC, Bailey A, Cox CJ, O'Neill MS, Schneider D, Steffen K and White JWC (2016) Surface-atmosphere decoupling limits accumulation at Summit, Greenland. *Science Advances,* **2**(4), e1501704 (doi: 10.1126/sciadv.1501704)

Bolzan J and Strobel M (1994) Accumulation-Rate Variations Around Summit, Greenland. *J.Glaciol.,* **40**(134), 56-66 (doi: 10.3189/S0022143000003798)

Box JE and Steffen K (2001) Sublimation on the Greenland ice sheet from automated weather station observations*. Journal of Geophysical Research-Atmospheres,* **106**(D24), 33965-33981 (doi: 10.1029/2001JD900219)

Box JE, Cressie N, Bromwich DH, Jung J, van den Broeke M, van Angelen JH, Forster RR, Miege C, Mosley-Thompson E, Vinther B and McConnell JR (2013) Greenland Ice Sheet Mass Balance Reconstruction. Part I: Net Snow Accumulation (1600-2009)*. J.Clim.,* **26**(11), 3919-3934 (doi: 10.1175/JCLI-D-12-00373.1)

Castellani BB, Shupe MD, Hudak DR and Sheppard BE (2015) The annual cycle of snowfall at Summit, Greenland*. Journal of Geophysical Research-Atmospheres,* **120**(13), 6654-6668 (doi: 10.1002/2015JD023072)

497   Cullather RI, Nowicki SMJ, Zhao B and Suarez MJ (2014) Evaluation of the Surface

498   Representation of the Greenland Ice Sheet in a General Circulation Model. *J.Clim.,* **27**(13),

499   4835-4856 (doi: 10.1175/JCLI-D-13-00635.1)

500   Dibb J and Fahnestock M (2004) Snow accumulation, surface height change, and firn

501   densification at Summit, Greenland: Insights from 2 years of in situ observation. *Journal of*

502   *Geophysical Research-Atmospheres,* **109**(D24), D24113 (doi: 10.1029/2003JD004300)

503   Fausto RS, Box JE, Vandecrux B, van As D, Steffen K, MacFerrin MJ, Machguth H, Colgan W,

504   Koenig LS, McGrath D, Charalampidis C and Braithwaite RJ (2018) A Snow Density Dataset for

505   Improving Surface Boundary Conditions in Greenland Ice Sheet Firn Modeling. *Frontiers in*

506   *Earth Science,* **6**, 51 (doi: 10.3389/feart.2018.00051)

507   Fettweis X, Franco B, Tedesco M, van Angelen JH, Lenaerts JTM, van den Broeke MR and

508   Gallee H (2013) Estimating the Greenland ice sheet surface mass balance contribution to future

509   sea level rise using the regional atmospheric climate model MAR. *Cryosphere,* **7**(2), 469-489

510   (doi: 10.5194/tc-7-469-2013)

511   Fettweis X, Hofer S, Krebs-Kanzow U, Amory C, Aoki T, Berends CJ, Born A, Box JE, Delhasse

512   A, Fujita K, Gierz P, Goelzer H, Hanna E, Hashimoto A, Huybrechts P, Kapsch M, King MD,

513   Kittel C, Lang C, Langen PL, Lenaerts JTM, Liston GE, Lohmann G, Mernild SH, Mikolajewicz

514   U, Modali K, Mottram RH, Niwano M, Noel B, Ryan JC, Smith A, Streffing J, Tedesco M, van de

515   Berg WJ, van den Broeke M, van de Wal RSW, van Kampenhout L, Wilton D, Wouters B,

516   Ziemen F and Zolles T (2020) GrSMBMIP: intercomparison of the modelled 1980-2012 surface

517   mass balance over the Greenland Ice Sheet. *Cryosphere,* **14**(11), 3935-3958 (doi: 10.5194/tc-

518   14-3935-2020)

519 Gallagher MR, Shupe MD, Chepfer H and L'Ecuyer T Relating snowfall observations to

520 Greenland ice sheet mass changes: an atmospheric circulation perspective. *The*

521 *Cryosphere,*(2), 435

522 Global Modeling and Assimilation Office (GMAO) (2015) MERRA-2 tavg3_2d_glc_Nx: 2d,3-

523 Hourly,Time-Averaged,Single-Level,Assimilation,Land Ice Surface Diagnostics V5.12.4,

524 Greenbelt, MD, USA, Goddard Earth Sciences Data and Information Services Center (GES

525 DISC) **2021**(Nov. 20)

526 Howat IM, de la Pena S, Desilets D and Womack G (2018) Autonomous ice sheet surface mass

527 balance measurements from cosmic rays. *Cryosphere,* **12**(6), 2099-2108 (doi: 10.5194/tc-12-

528 2099-2018)

529 Kuipers Munneke P, Ligtenberg SRM, Noël BPY, Howat IM, Box JE, Mosley-Thompson E,

530 McConnell JR, Steffen K, Harper JT, Das SB and van den Broeke MR (2015) Elevation change

531 of the Greenland Ice Sheet due to surface mass balance and firn processes, 1960–2014. The

532 Cryosphere,(6), 2009

533 Lenaerts JTM, van den Broeke MR, van Angelen JH, van Meijgaard E and Dery SJ (2012)

534 Drifting snow climate of the Greenland ice sheet: a study with a regional climate model.

535 *Cryosphere,* **6**(4), 891-899 (doi: 10.5194/tc-6-891-2012)

536 Lenaerts JTM, Medley B, van den Broeke MR and Wouters B (2019) Observing and Modeling

537 Ice Sheet Surface Mass Balance. *Rev.Geophys.,* **57**(2), 376-420 (doi: 10.1029/2018RG000622)

538 McIlhattan EA, Pettersen C, Wood NB and L'Ecuyer TS (2020) Satellite observations of snowfall

539 regimes over the Greenland Ice Sheet. *Cryosphere,* **14**(12), 4379-4404 (doi: 10.5194/tc-14-

540 4379-2020)

541   Montgomery L, Koenig L, Lenaerts JTM and Kuipers Munneke P (2020) Accumulation rates

542   (2009-2017) in Southeast Greenland derived from airborne snow radar and comparison with

543   regional climate models. *Annals of Glaciology,* **61**(81), 225-233 (doi: 10.1017/aog.2020.8)

544   Overly TB, Hawley RL, Helm V, Morris EM and Chaudhary RN (2016) Greenland annual

545   accumulation along the EGIG line, 1959-2004, from ASIRAS airborne radar and neutron-probe

546   density measurements. *Cryosphere,* **10**(4), 1679-1694 (doi: 10.5194/tc-10-1679-2016)

547   Pettersen C, Bennartz R, Merrelli AJ, Shupe MD, Turner DD and Walden VP (2018)

548   Precipitation regimes over central Greenland inferred from 5 years of ICECAPS observations.

549   *Atmospheric Chemistry and Physics,* **18**(7), 4715-4735 (doi: 10.5194/acp-18-4715-2018)

550   IMBIE Team (2020) Mass balance of the Greenland Ice Sheet from 1992 to 2018.

551   *Nature,* **579**(7798), 233-+ (doi: 10.1038/s41586-019-1855-2)

552   Sheppard BE and Joe PI (2008) Performance of the precipitation occurrence sensor system as

553   a precipitation gauge. *J.Atmos.Ocean.Technol.,* **25**(2), 196-212 (doi:

554   10.1175/2007JTECHA957.1)

555   Sturm M, Taras B, Liston GE, Derksen C, Jonas T and Lea J (2010) Estimating Snow Water

556   Equivalent Using Snow Depth Data and Climate Classes. *J.Hydrometeorol.,* **11**(6), 1380-1394

557   (doi: 10.1175/2010JHM1202.1)

558   Tedesco M and Fettweis X (2020) Unprecedented atmospheric conditions (1948-2019) drive the

559   2019 exceptional melting season over the Greenland ice sheet. *Cryosphere,* **14**(4), 1209-1223

560   (doi: 10.5194/tc-14-1209-2020)

561   Wayand NE, Massmann A, Butler C, Keenan E, Stimberis J and Lundquist JD (2015) A

562   meteorological and snow observational data set from Snoqualmie Pass (921 m), Washington

563   Cascades, USA. *Water Resour.Res.,* **51**(12), 10092-10103 (doi: 10.1002/2015WR017773)

564   Zwally HJ and Li J (2002) Seasonal and interannual variations of firn densification and ice-sheet

565   surface elevation at the Greenland summit. *J. Glaciol.,* **48**, 199-207

566

567

568

569

570

571

572

573

574

575

576

577

578

FIGURE CAPTIONS

Fig. *1*. Time series of snow board (A) sample snow depth, as measured from the surface to the board, and (B) sample snow water equivalent (SWE) thickness, obtained from average of sample mass and volume measurements. Dashes denote transitions in sampling sites.

Fig. *2*. (A) Cumulative SWE thickness obtained from differencing concurrent measurements between sample sites (i.e., tie-point measurements). (B) Same as in (A) but with a rate of 24 cm w.e. a^{-1} subtracted. (C) 7-day change in SWE between measurements. Dashes denote changes in sampling board sites. (D) Sample density obtained by dividing SWE by the snow depth.

Fig. *3*. Comparison of snow sample depth to density. Color scale is sample observation date.

Fig. *4*. Change in snow depth versus change in SWE between observations. Outliers are marked in red with observation dates. The precision of snow depth measurements is 0.5 cm. Black curve is the best fit line, corresponding to a density of 0.278 g cm^{-3}.

Fig. *5*. (A) Cumulative change in (black) surface height measured at the snow stake network and (gray) snow board sample thickness. (B) Same as (A) with best fit linear trend removed.

**Fig. *6*.** (A) Cumulative SWE and (B) detrended cumulative SWE measured from the (black) Precipitation Occurrence Sensor System (POSS) and (gray) Snow Board. (C) Scatter plot of changes in SWE from the POSS and Snow Board measured between snow board observations. Black curve is the line of best fit with the equation in legend.

Fig. *7*. (A) Cumulative and (B) detrended SWE from (black curve) MERRA-2 and (dashes) MAR reanalysis model outputs and (gray) Snow Board observations. (C) Same as (B) but with gray curve as cumulative SWE estimated from the average of the snow stake network adjusted using a density of 0.3 g cm^{-3}.
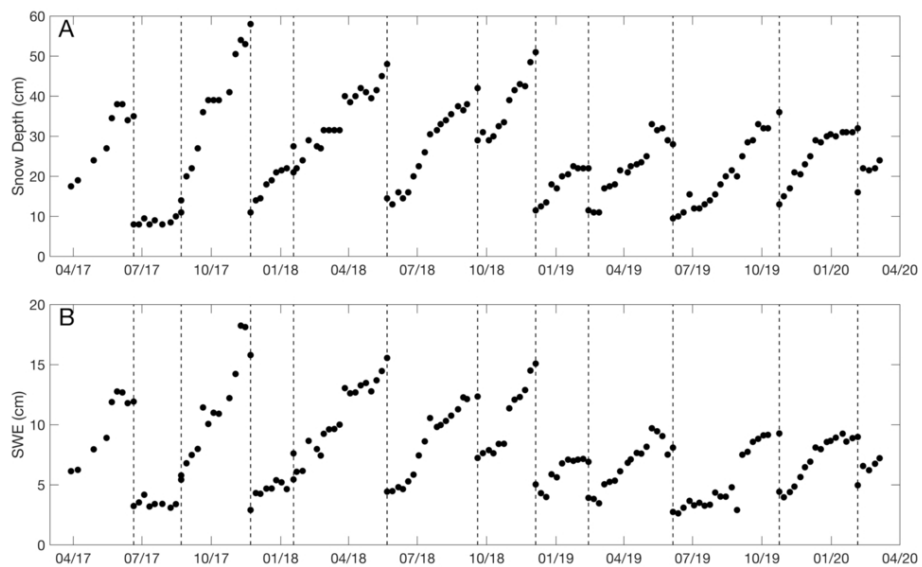
Time series of snow board (A) sample snow depth, as measured from the surface to the board, and (B) sample snow water equivalent (SWE) thickness, obtained from average of sample mass and volume measurements. Dashes denote transitions in sampling sites.

178x107mm (150 x 150 DPI)
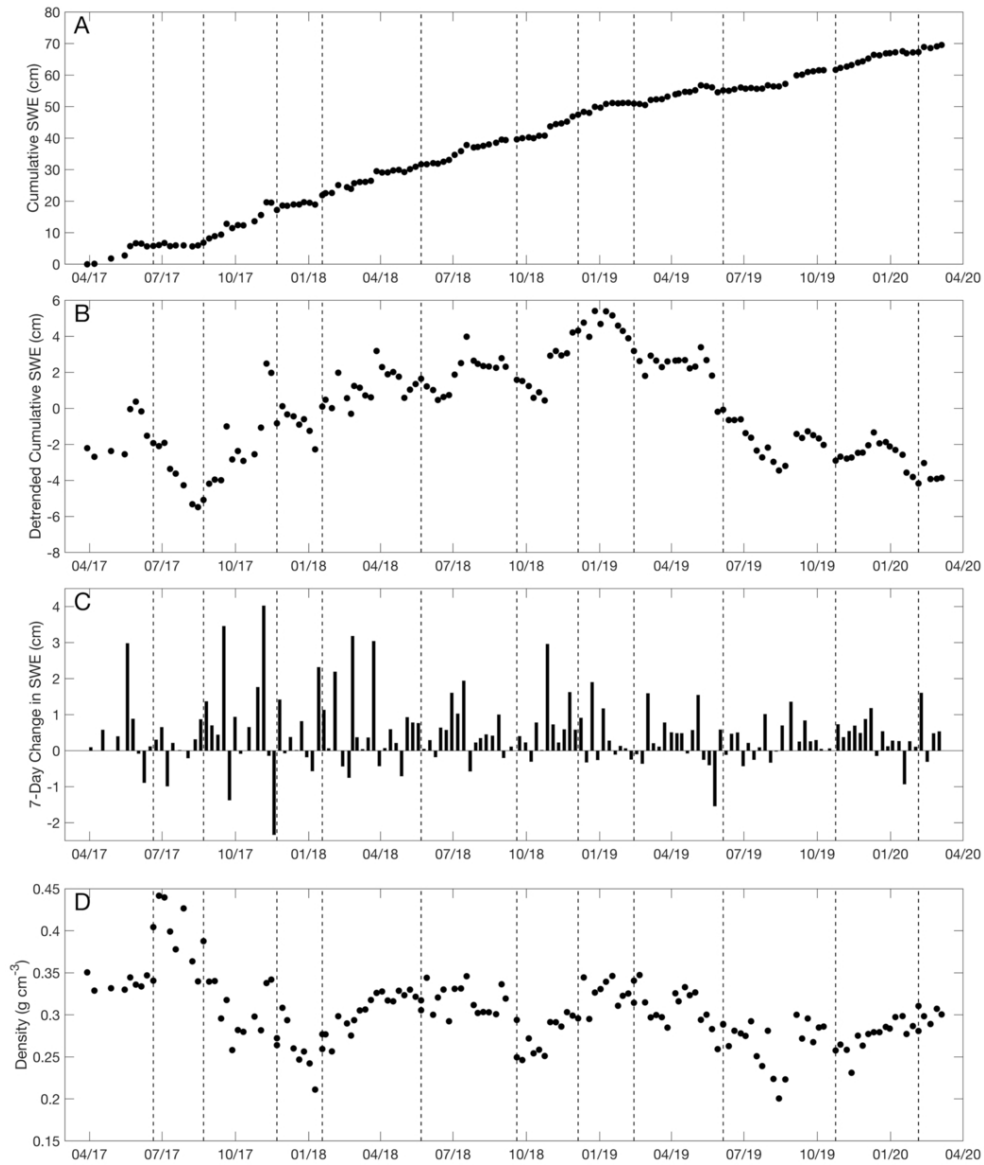
(A) Cumulative SWE thickness obtained from differencing concurrent measurements between sample sites (i.e., tie-point measurements). (B) Same as in (A) but with a rate of 24 cm w.e. a-1 subtracted. (C) 7-day change in SWE between measurements. Dashes denote changes in sampling board sites. (D) Sample density obtained by dividing SWE by the snow depth.
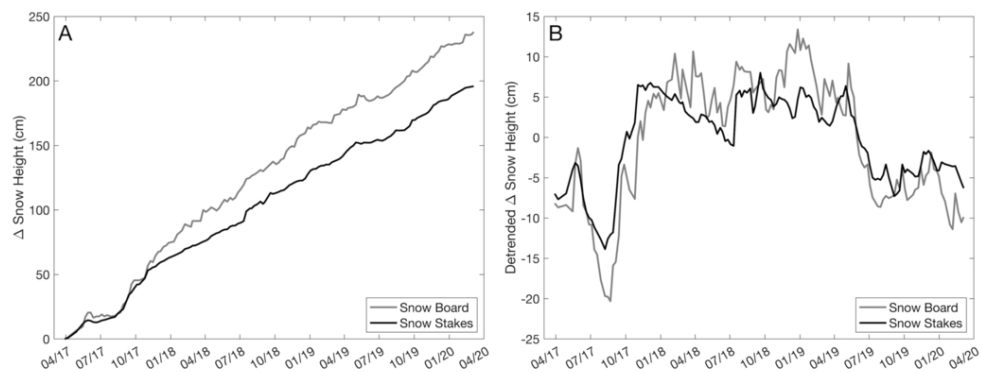
178x214mm (150 x 150 DPI)
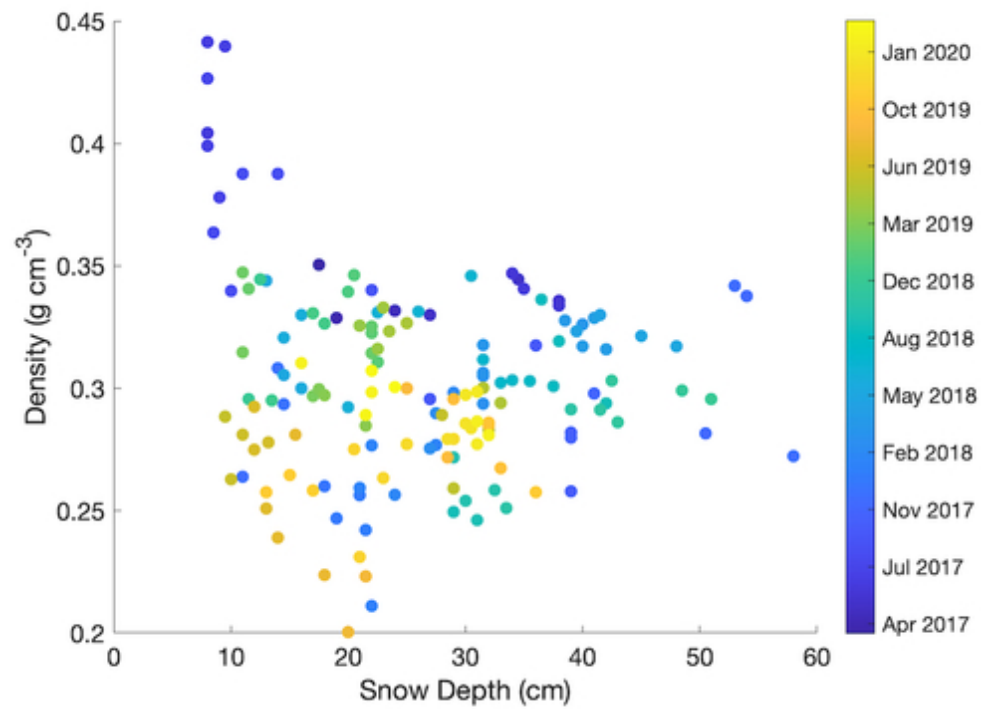
Comparison of snow sample depth to density. Color scale is sample observation date.

85x63mm (150 x 150 DPI)
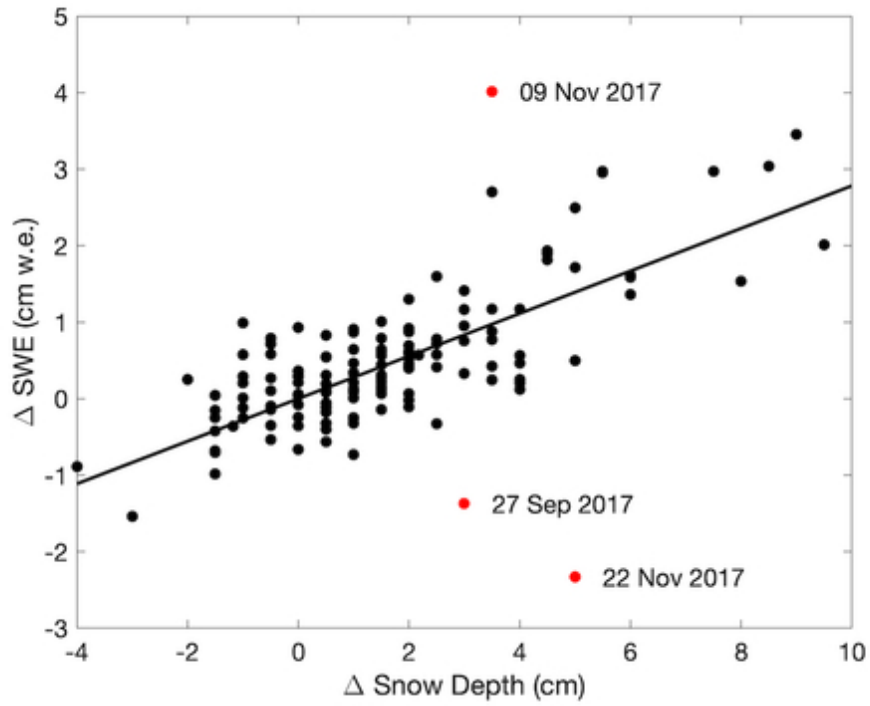
Change in snow depth versus change in SWE between observations. Outliers are marked in red with observation dates. The precision of snow depth measurements is 0.5 cm. Black curve is the best fit line, corresponding to a density of 0.278 g cm-3.

85x63mm (150 x 150 DPI)

(A) Cumulative change in (black) surface height measured at the snow stake network and (gray) snow board sample thickness. (B) Same as (A) with best fit linear trend removed.

178x67mm (150 x 150 DPI)
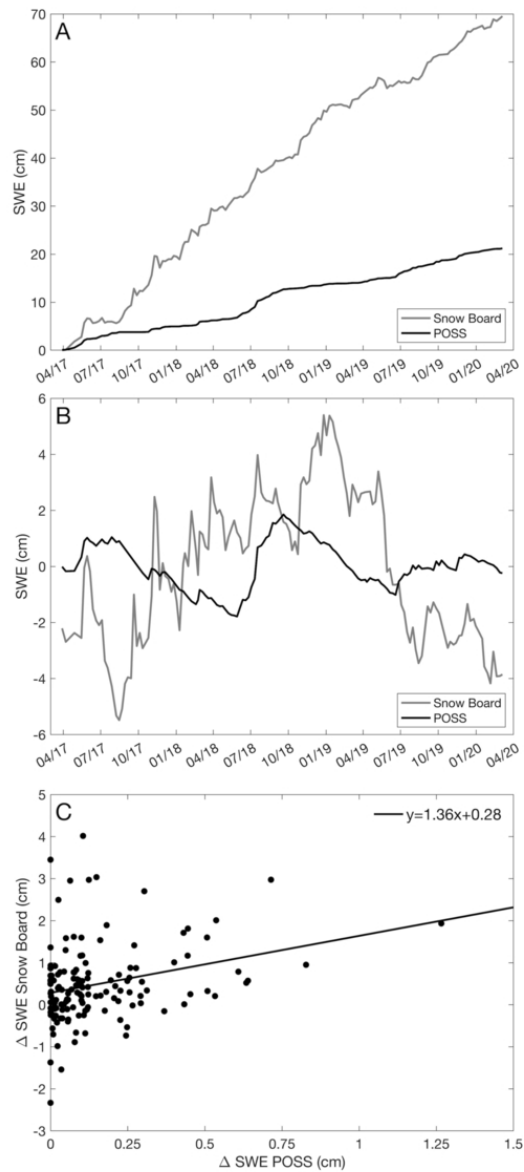
(A) Cumulative SWE and (B) detrended cumulative SWE measured from the (black) Precipitation Occurrence Sensor System (POSS) and (gray) Snow Board. (C) Scatter plot of changes in SWE from the POSS and Snow Board measured between snow board observations. Black curve is the line of best fit with the equation in legend.

85x193mm (150 x 150 DPI)
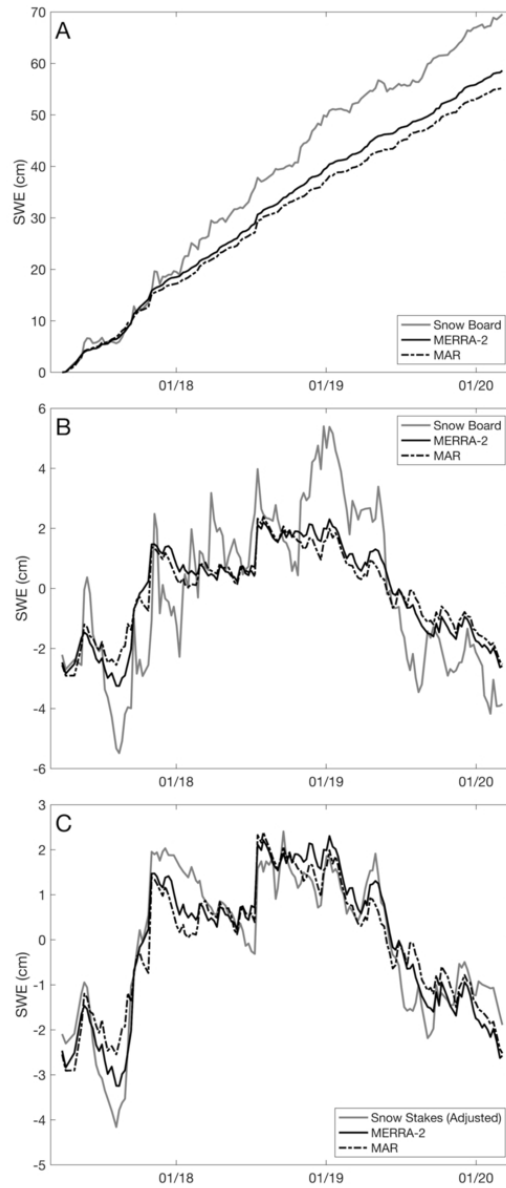
(A) Cumulative and (B) detrended SWE from (black curve) MERRA-2 and (dashes) MAR reanalysis model outputs and (gray) Snow Board observations. (C) Same as (B) but with gray curve as cumulative SWE estimated from the average of the snow stake network adjusted using a density of 0.3 g cm-3.

85x193mm (150 x 150 DPI)